

## Simulation of Jet Breakup in Lower Plenum with Internal Structure Using Smoothed Particle Hydrodynamics

Hoon Chae, So-Hyun Park, Eung Soo Kim\*

Department of Nuclear Engineering, Seoul National University

\*Corresponding author: kes7741@snu.ac.kr

### 1. Introduction

Jet breakup is an early stage of Fuel Coolant Interaction(FCI) that occurs when molten corium penetrates into the coolant during a severe accident of a nuclear power plant. Since the jet breakup pattern affects the results of steam explosion, debris formation and coolability, deep understanding of this phenomenon is needed.

Saito et al. [1, 2] conducted experiments on the hydrodynamic behavior of jets in the presence of complicate structures such as control rods guide tubes(CRGTs) and control rod drive housings in the lower plenum of the BWR, the reactor type of the Fukushima Daiichi nuclear power plant accident.

Suzuki et al. [3] performed numerical simulation on this experiment by improving interface tracking method code TPFIT(Two-Phase Flow simulation code with Interface Tracking). They showed that the method can qualitatively simulate the jet breakup phenomena in the complicate structures.

Smoothed Particle Hydrodynamics (SPH) is a Lagrangian-based computational method. The fluid is composed by particles without the use of a lattice to interpreting each particle's movement as an interaction with neighbor particles. Especially, it is effective for free surface flow and multiphase flow analysis because there is no need to track interface.

Park et al. [4] simulated the experiment of injecting water jet into simulant pool with SPH, and accurately resolved the physical features of the jet breakup phenomenon.

In this study, the SOPHIA code using the SPH method developed by Seoul National University was used. With the code, the hydraulic behavior of the jet in the presence of complicate structures is simulated.

Through the analysis, we find the applicability of the SPH method to jet falling behavior of FCI, one of the severe accident phenomena.

### 2. SPH Methodology

In this section, the basic concepts and methodologies of SPH mentioned above is covered.

#### 2.1 SPH basics

The basic idea of SPH is to represent arbitrary functions using kernel functions that approximate delta functions and integral interpolant. Since the fluid is discretized into particles, the summation interpolant is applied as Eq. (1).

$$f(\mathbf{x}_i) = \sum_j \frac{m_j}{\rho_j} f(\mathbf{x}_j) W(\mathbf{x}_i - \mathbf{x}_j, h) \quad (1)$$

Where  $i, j$  denote center particle and neighbor particle and  $m, \rho$  denote mass and density of particle.  $W$  is the kernel function and  $h$  is the smoothing length that determines the influence distance of the  $W$ . The kernel function is a function of the distance between particles. The value is highest at the center and smoothly decrease as distance from the center is increase.

Spatial derivative approximations for arbitrary functions can be obtained by differentiating the kernel function.[4]

$$\nabla f(\mathbf{x}_i) = \sum_j \frac{m_j}{\rho_j} f(\mathbf{x}_j) \nabla W(\mathbf{x}_i - \mathbf{x}_j, h) \quad (2)$$

#### 2.2 Governing equations

The governing equations of SPH are mass conservation, momentum equation and equation of state(EOS). Energy conservation is omitted because it is not a consideration in this study. The mass conservation law is the continuity equation.

$$\frac{D\rho}{Dt} + \rho \nabla \cdot \mathbf{u} = 0 \quad (3)$$

$\mathbf{u}$  in Eq. (3) is velocity. Since SPH tracks the movement of the mass, conservation of mass is naturally established. Eq. (3) can be used to calculate particle density in SPH. The momentum equation uses the Navier-Stokes equation.

$$\frac{D\mathbf{u}}{Dt} = -\frac{\nabla p}{\rho} + \nu \nabla^2 \mathbf{u} + \mathbf{g} \quad (4)$$

Where  $\nu$  is kinematic viscosity and  $\mathbf{g}$  is gravitational acceleration. Each term on the right side means the acceleration by pressure force, viscous force, gravity force in order.

Weakly Compressible SPH(WCSPH) was used in this study. The following Tait equation is used as EOS to close the governing equation assuming weak compressibility [5].

$$p = \frac{c_0^2 \rho_0}{\gamma} \left[ \left( \frac{\rho}{\rho_0} \right)^\gamma - 1 \right] \quad (5)$$

$c_0, \rho_0$  denote the speed of sound and reference density.  $\gamma(=7)$  is the polytrophic constant that determines the sensitivity of pressure calculation

### 2.3 SPH formulations

There are two methods for calculating density in SPH. Mass summation method by smoothing with neighbor particles directly using Eq. (1) and continuity equation method by calculating time derivative of density. The mass summation method is used as below.

$$\rho_i = \sum_j m_j W(\mathbf{x}_i - \mathbf{x}_j, h) \quad (6)$$

Each term in Eq. (4) is represented by the SPH formulation as follows.

$$\left(\frac{D\mathbf{u}}{Dt}\right)_i = -\sum_j m_j \left(\frac{p_i}{\rho_i^2} + \frac{p_j}{\rho_j^2}\right) \nabla W(\mathbf{x}_{ij}, h) \quad (7)$$

$$\left(\frac{D\mathbf{u}}{Dt}\right)_i = \sum_j \frac{4m_j}{\rho_i \rho_j} \frac{\mu_i \mu_j}{\mu_i + \mu_j} \frac{\mathbf{x}_{ij} \mathbf{u}_{ij}}{(|\mathbf{x}_{ij}|^2 + \eta^2)} \nabla W(\mathbf{x}_{ij}, h) \quad (8)$$

Where  $\mathbf{x}_{ij} = \mathbf{x}_i - \mathbf{x}_j$ ,  $\mathbf{u}_{ij} = \mathbf{u}_i - \mathbf{u}_j$  and  $\mu$  is dynamic viscosity. Eq. (7) is the acceleration due to the pressure force while Eq. (8) due to viscous force.

Macroscopic continuum surface force(CSF) model was used for calculating surface tension.[6]

$$\left(\frac{D\mathbf{u}}{Dt}\right)_i = -\frac{\sigma}{\rho_i} \kappa_i (\nabla c)_i \quad (9)$$

$$\mathbf{n}_i = (\nabla c)_i = \frac{1}{V_i} \sum_j (V_i^2 + V_j^2) \frac{c_i^j + c_j^i}{2} \nabla W(\mathbf{x}_{ij}, h) \quad (10)$$

$$\kappa_i = -\nabla \cdot \left(\frac{\mathbf{n}_i}{|\mathbf{n}_i|}\right) = -n \frac{\sum_j V_j \left(\frac{\mathbf{n}_i}{|\mathbf{n}_i|} - \varphi_{ij} \frac{\mathbf{n}_j}{|\mathbf{n}_j|}\right) \cdot \nabla W(\mathbf{x}_{ij}, h)}{\sum_j V_j |\mathbf{x}_{ij}| |\nabla W(\mathbf{x}_{ij}, h)|} \quad (11)$$

Where  $\sigma, \kappa, c, V$  denote surface tension coefficient, curvature, color field, volume of the particle.  $\varphi$  is a parameter which is 0 if  $i$  and  $j$  are the same phase, otherwise 1.

### 3. Simulation Set-up

In this study, the jet breakup in the presence of complicate structures was simulated by the SPH methodology. Experiments that observed jet breakup behavior in the multi-channel of the BWR lower plenum conducted in Saito et al. [1, 2] were selected as a reference. An experimental case using a jet of FC-3283 material with a diameter of 7 mm and the injection speed of  $2.12 \pm 0.03$  m/s was simulated.

#### 3.1 Reference experiment set-up

As shown in Figure 1, the experimental apparatus consists of a test section filled with water and a steady jet injection equipment that is filled with simulant and constantly ejects them.

The test section contains 32 structures that simulate the CRGTs and the control rod drive housings as shown in Figure 2.

A jet was injected through the nozzle into the middle of the four CRGTs. Water was filled up to the level of the core support plate, assuming that the core support plate failed just below the damaged fuel assembly.

The experiment was conducted at room temperature and atmospheric pressure. The physical properties of the simulant are shown in Table I.

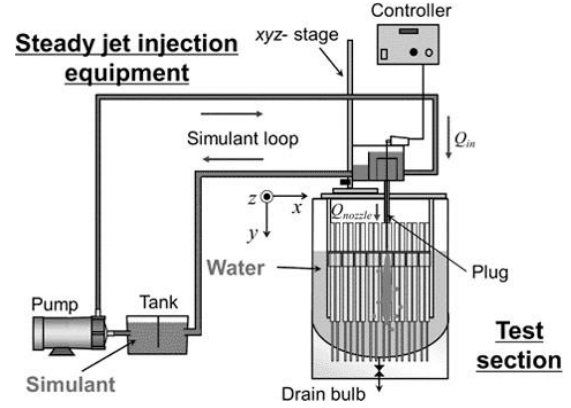


Figure 1. Schematic diagram of the experimental apparatus [2]

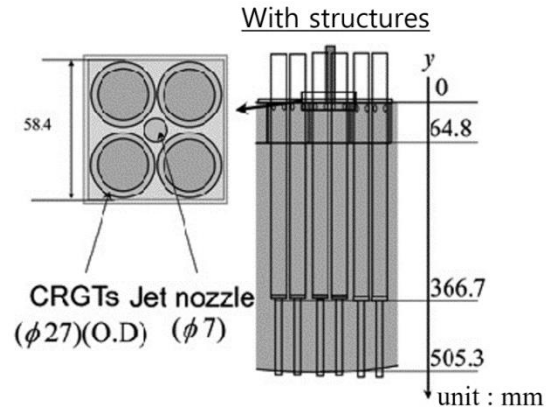


Figure 2. Test section condition [2]

Table I. Physical properties of Fluorinert™ (FC-3283) [2]

Density (kg/m <sup>3</sup> )	Surface tension (N/m)	Kinematic viscosity (mm <sup>2</sup> /s)
1830	0.040	0.82

#### 3.2 SPH simulation set-up

To simulate the reference experiments, a 3D structure of  $200 \times 150 \times 500$  (mm) was formed as shown in Figure 3. 12 complicate structures were located. Jet was injected into the center of the four CRGTs in the middle and had a constant velocity before reaching the surface. A total of 16,349,264 particles were used in the calculation and the initial particle distance was 1mm. The physical properties of the particles of simulant and water were same as the experiment. The time-step was

$2.0 \times 10^{-6}$  s and total calculation time was 1 s. The sound speed 50 m/s and Wendland2 kernel were used.

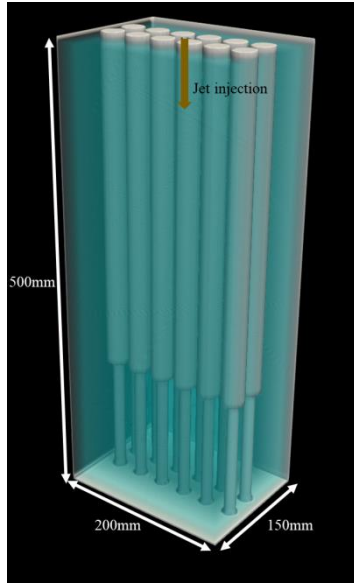


Figure 3. Simulation configuration

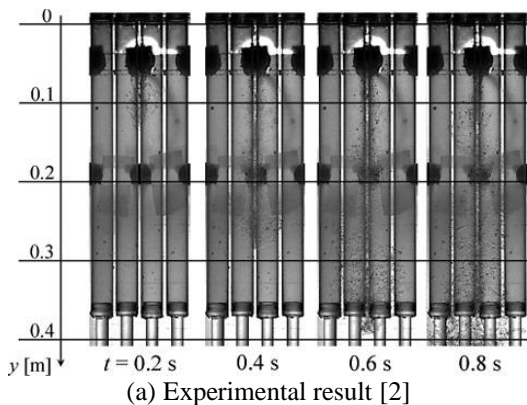
#### 4. Result and Discussions

##### 4.1 Jet falling behavior

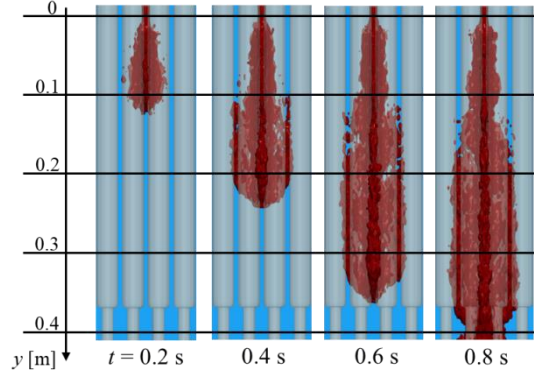
Figure 4 shows the jet falling behavior of the experiment (a) and SPH simulation (b). From the Figure 4, we can see that the SPH simulation predicts the experiment well.

For a more quantitative comparison, the front position of the jet over time is shown in Figure 5, along with the experimental data and the simulation result of Suzuki et al. [3]. Because there is a slight difference in the injection mode in the experiment and simulations, the moment when the jet passes 0.1 m is defined as 0 s. As can be seen from the Figure 5, SPH simulation predicted jet front position better than the previous simulation.

Figure 6 shows the velocity of the jet front over time. Previous simulations underestimated the velocity, while SPH simulation slightly overestimate the velocity later, but similar result was obtained.



(a) Experimental result [2]



(b) SPH simulation result

Figure 4. Jet falling behavior

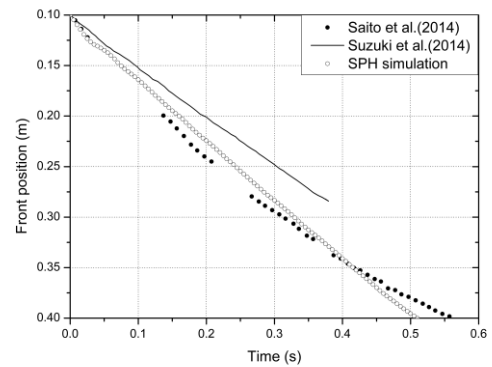


Figure 5. Front position comparison of the experiment and simulations

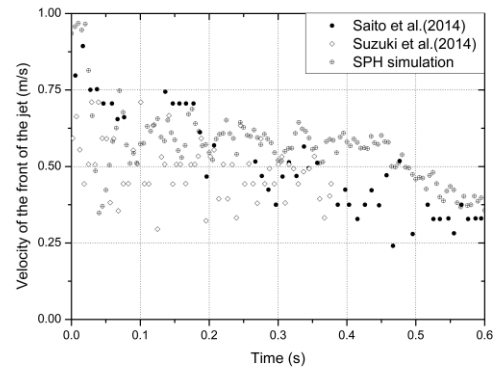


Figure 6. Velocity of jet front comparison of the experiment and simulations

##### 4.2 Jet expansion behavior

According to Saito et al. (2016), jet expansion behavior is suppressed in the presence of the complicate structures. Figure 7 shows the time-averaged result of velocity profiles outside the jet for the presence of the structures obtained by PIV method and SPH simulation at the position  $y = 10$  mm. Closed and open plots are experiment and SPH simulation case, respectively.

As shown in the figure, the x direction velocity is negative due to the pressure difference. In addition, if there are structures, the flow is confined by the structures and the expansion is restricted. So, there is tendency to flow towards the mainstream. Especially this phenomenon can be seen well near the 15.7 mm position where structures are closest. This phenomenon is also observed in SPH simulation. As with the experimental results, the expansion was confined by the structures, especially around 15.7 mm.

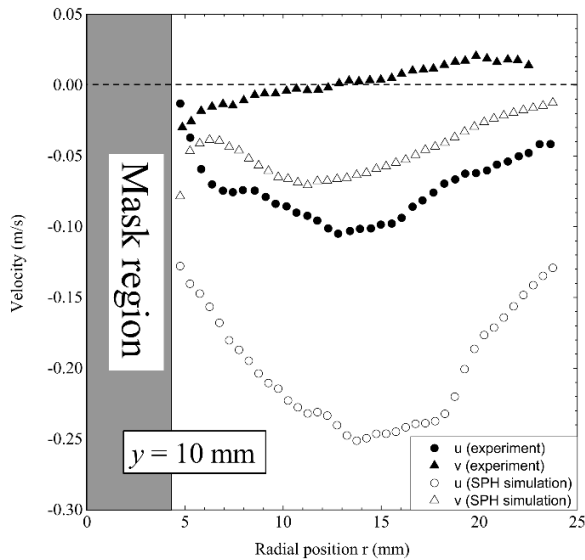


Figure 7. External velocity profiles of the jet

Additionally, the velocity field in the horizontal direction can be also seen from the simulation as shown in Figure 8, while only the vertical velocity field can be seen from the experiment. From the horizontal vector fields around the jet at  $y = 10$  mm, the flow is directed in the mainstream region. This also shows that the expansion of the jet is restricted by the structures.

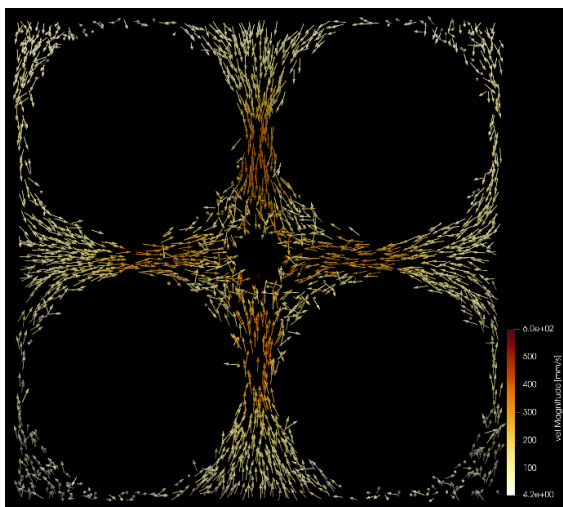


Figure 8. External velocity field of jet ( $y = 10$ mm)

## 5. Summary

In this study, the experiment conducted by Saito et al. [1, 2] was simulated by the SPH method. Jet behavior was observed in the apparatus of the BWR lower plenum with complicate structures. For the SPH analysis, SOPHIA code developed by Seoul National University was used. From the results of the front position of jet over time, SPH simulation shows better agreement with the experimental results than previous numerical simulation. By checking the velocity profile and velocity field around the jet, the effect of suppressing jet expansion by the structures was also observed. We find applicability of the SPH method to simulate the jet falling behavior in the nuclear reactor.

## ACKNOWLEDGEMENT

This research was supported by Nuclear Energy Technology Development Program(U.S.-ROK I-NERI Program) through the National Research Foundation of Korea(NRF) funded by the Ministry of Science and ICT(NRF-2019M2A8A1000630)

## REFERENCES

- [1] Saito, Ryusuke, Yutaka Abe, and Hiroyuki Yoshida. "Experimental study on breakup and fragmentation behavior of molten material jet in complicated structure of BWR lower plenum." *Journal of Nuclear Science and Technology* 51.1 (2014): 64-76.
- [2] Saito, Ryusuke, Yutaka Abe, and Hiroyuki Yoshida. "Breakup and fragmentation behavior of molten material jet in multi-channel of BWR lower plenum." *Journal of Nuclear Science and Technology* 53.2 (2016): 147-160.
- [3] Suzuki, Takayuki, Hiroyuki Yoshida, and Fumihisa Nagase. "Development of numerical evaluation method for fluid dynamics effects on jet breakup phenomena in BWR lower plenum." *Journal of Nuclear Science and Technology* 51.7-8 (2014): 968-976.
- [4] Park, S. H., Jo, Y. B., Kim, E. S. High Resolution 3D Simulation of Melt Jet Breakup Phenomenon Using Multi-GPU-Based Smoothed Particle Hydrodynamics Code and Comparison with Experimental Result. In *ASME 2020 Power Conference*. American Society of Mechanical Engineers Digital Collection.
- [5] Monaghan, Joe J. "Smoothed particle hydrodynamics." *Annual review of astronomy and astrophysics* 30.1 (1992): 543-574.
- [6] Adami, S., X. Y. Hu, and Nikolaus A. Adams. "A new surface-tension formulation for multi-phase SPH using a reproducing divergence approximation." *Journal of Computational Physics* 229.13 (2010): 5011-5021.